Supporting Online Material for

KLF Family Members Regulate Intrinsic Axon Regeneration Ability

Darcie L. Moore, Murray G. Blackmore, Ying Hu, Klaus H. Kaestner, John L. Bixby, Vance P. Lemmon, Jeffrey L. Goldberg*

*To whom correspondence should be addressed. E-mail: jgoldberg@med.miami.edu

Published 9 October 2009, *Science* **326**, 298 (2009)
DOI: 10.1126/science.1175737

This PDF file includes:

Table of Contents

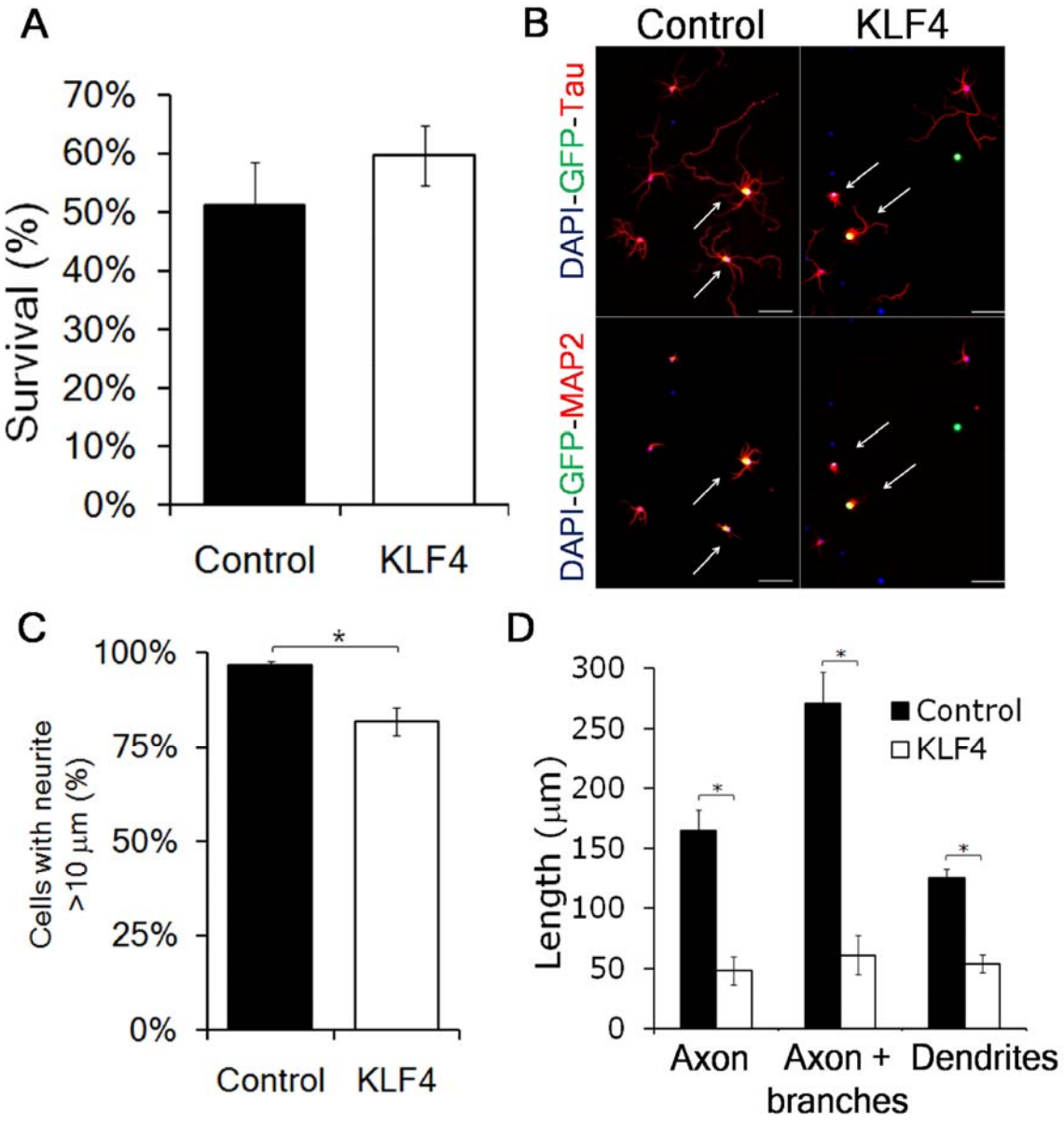

Figure S1. KLF4 overexpression in hippocampal neurons decreases neurite growth and neurite initiation. A-D) E18 hippocampal neurons were co-transfected with KLF4 or control plus EGFP, cultured on laminin-coated plates, and immunostained for Tau (neurites) and MAP2 (dendrites). A) There was no difference in survival by nuclear morphology and DAPI intensity between control- and KLF4-transfected neurons (Mean ± SD). B) Transfected EGFP+ cells (arrows) were imaged to detect DAPI, EGFP, and either Tau (top) or MAP2 (bottom). KLF4-transfected neurons had shorter axons and dendrites. (Scale bar, 50µm) C) KLF4 overexpression decreased the percentage of transfected neurons that were able to extend at least 1 neurite >10 µm (N=5; * $p<0.01$, paired t-test; mean ± SEM). D) KLF4 overexpression decreased both axon (Tau+/MAP2-) and dendrite (MAP2+) length (* $p<0.01$, t-test; mean ± SEM).

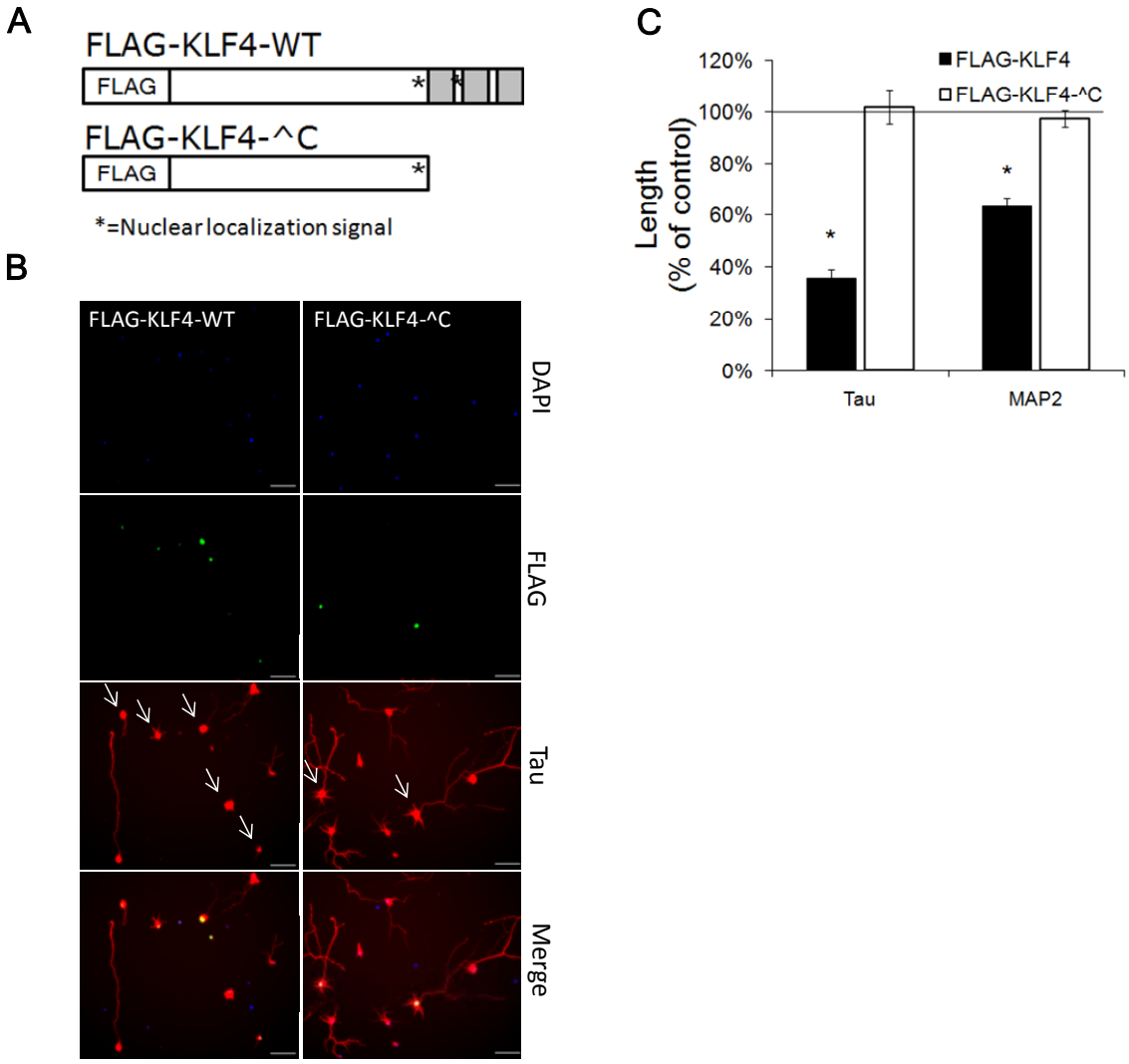

<u>Figure S2.</u> KLF4-mediated suppression of neurite growth requires the C-terminal zinc finger domain. E18 hippocampal neurons were transfected with either FLAG-KLF4-WT, FLAG-KLF4-^C lacking the C-terminal zinc finger DNA binding domain (A), or mCherry-pIRES2-eGFP as control. B) After 3DIV, neurons were stained for Tau (neurites) and MAP2 (dendrites) prior to imaging and analysis (Cellomics KSR). Transfected neurons are indicated by arrows. C) Neurite growth was normalized to control transfected neurons (not graphed, equal to 100%). WT KLF4 overexpression significantly decreased neurite growth in both Tau stained and MAP2 stained neurites, while deletion of KLF4's C-terminus led to growth indistinguishable from that of controls (* $p<0.01$, one representative experiment of 2 shown; mean ± SEM).

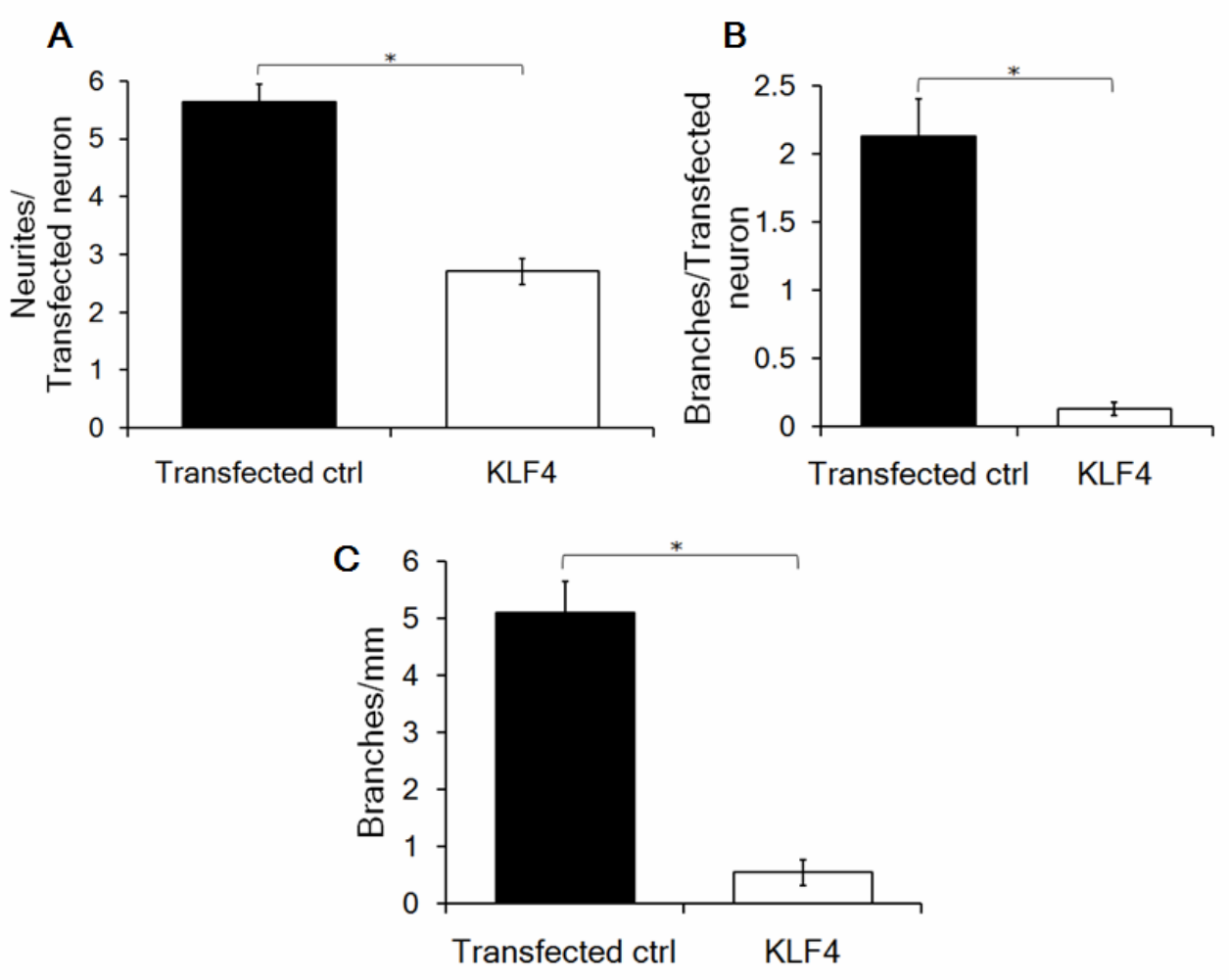

Figure S3. KLF4 overexpression decreases numbers of both neurites and branches in embryonic hippocampal neurons. E18 hippocampal neurons were electroporated with EGFP and either KLF4 or a pcDNA3 vector control and cultured for 3 days on PDL- and laminin-coated plates in growth media. Following immunostaining, transfected neurons were imaged and hand-traced. There was a decrease in the number of neurites originating from the cell body (A), the number of branches from all neurites (B), and the number of branches normalized to the total neurite length for each transfected neuron (C) after KLF4 overexpression (*$p<0.001$ for each graph, unpaired t-test; $n>50$ per condition; mean ± SEM).

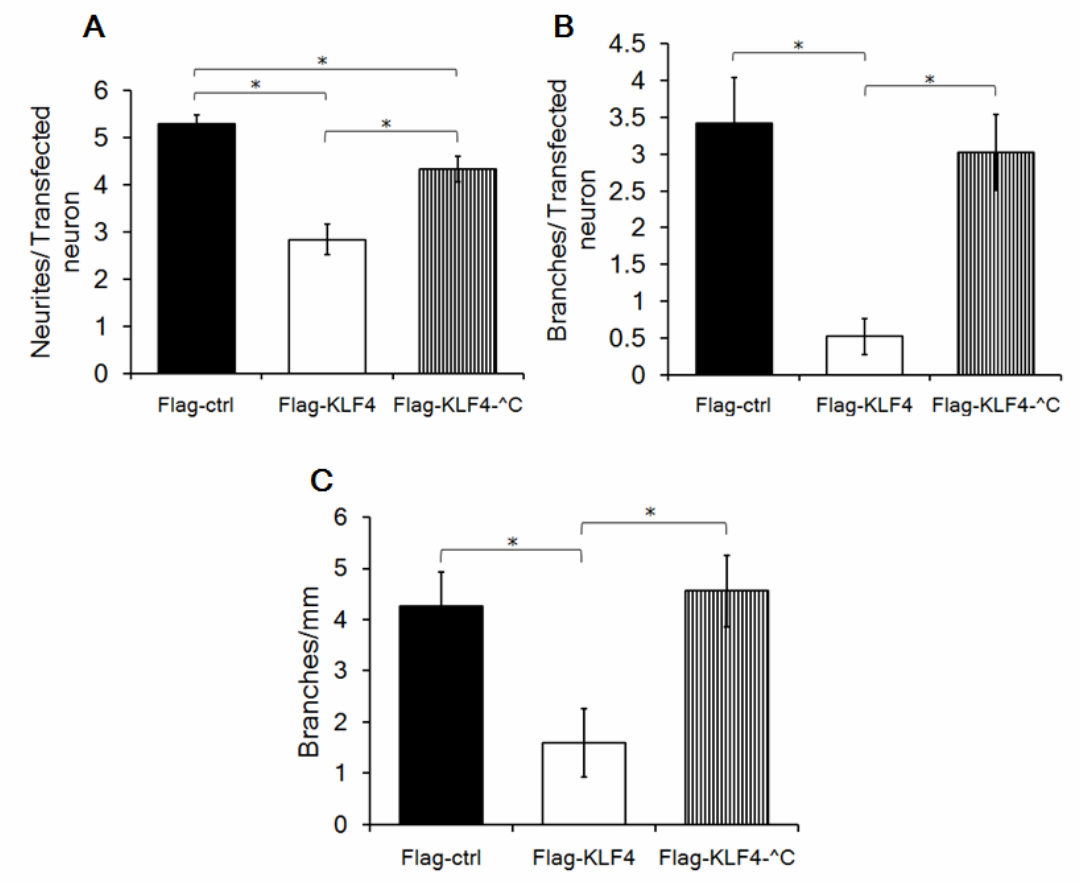

Figure S4. KLF4 overexpression in embryonic RGCs decreases the numbers of both neurites and branches. E20 RGCs were purified and transfected using Lipofectamine 2000 with a FLAG control plasmid, FLAG-KLF4, or FLAG-KLF4-^C deletion mutant lacking the C-terminal zinc finger DNA-binding domain. Neurons were plated for 3 days on PDL- and laminin-coated plates in growth media. Following immunostaining, transfected neurons were imaged and hand-traced. KLF4 overexpression decreased the average number of neurites (A), branches (B), and branches normalized to total neurite length of each neuron (C), whereas RGCs overexpressing the truncated Flag-KLF4-^C behaved similarly to controls ($p<0.01$, unpaired t-test post-Bonferroni; $n>25$ for each; mean ± SEM).

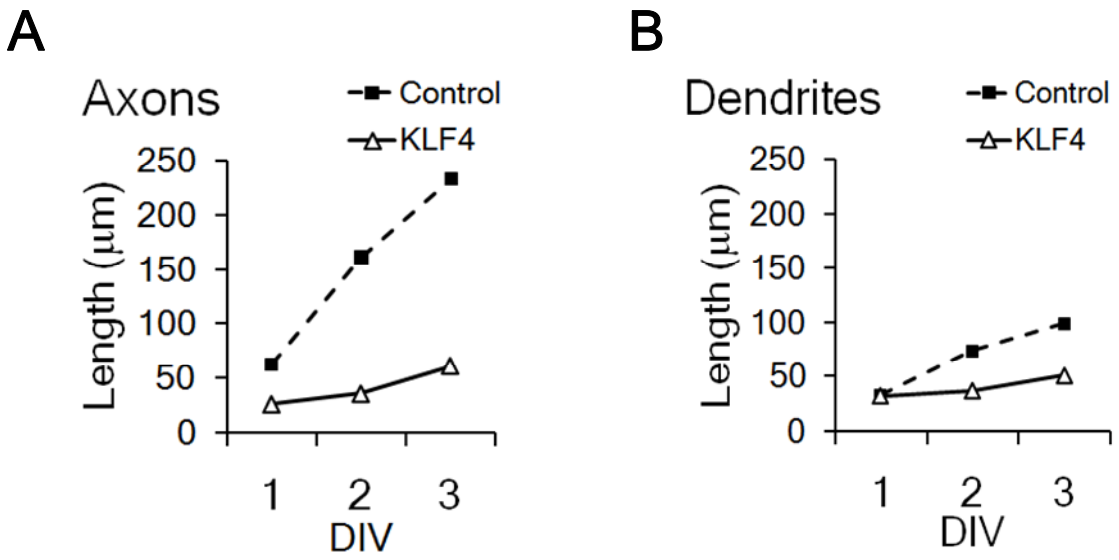

Figure S5. RGCs overexpressing KLF4 continue to extend neurites, but at a slower rate. E20 RGCs were purified and transfected with either KLF4-pIRES2-eGFP or mCherry-pIRES2-eGFP and cultured for 1, 2, or 3 days (DIV) prior to immunostaining for Tau and MAP2. Hand tracing revealed that while KLF4 transfected cells have decreased growth ability, they are still able to grow over a period of days whether looking at axon length (Tau+, MAP2-, A) or dendrite length (Tau+,MAP2+, B) (*$p<0.003$, unpaired t-tests comparing 1 to 3 DIV for each condition).

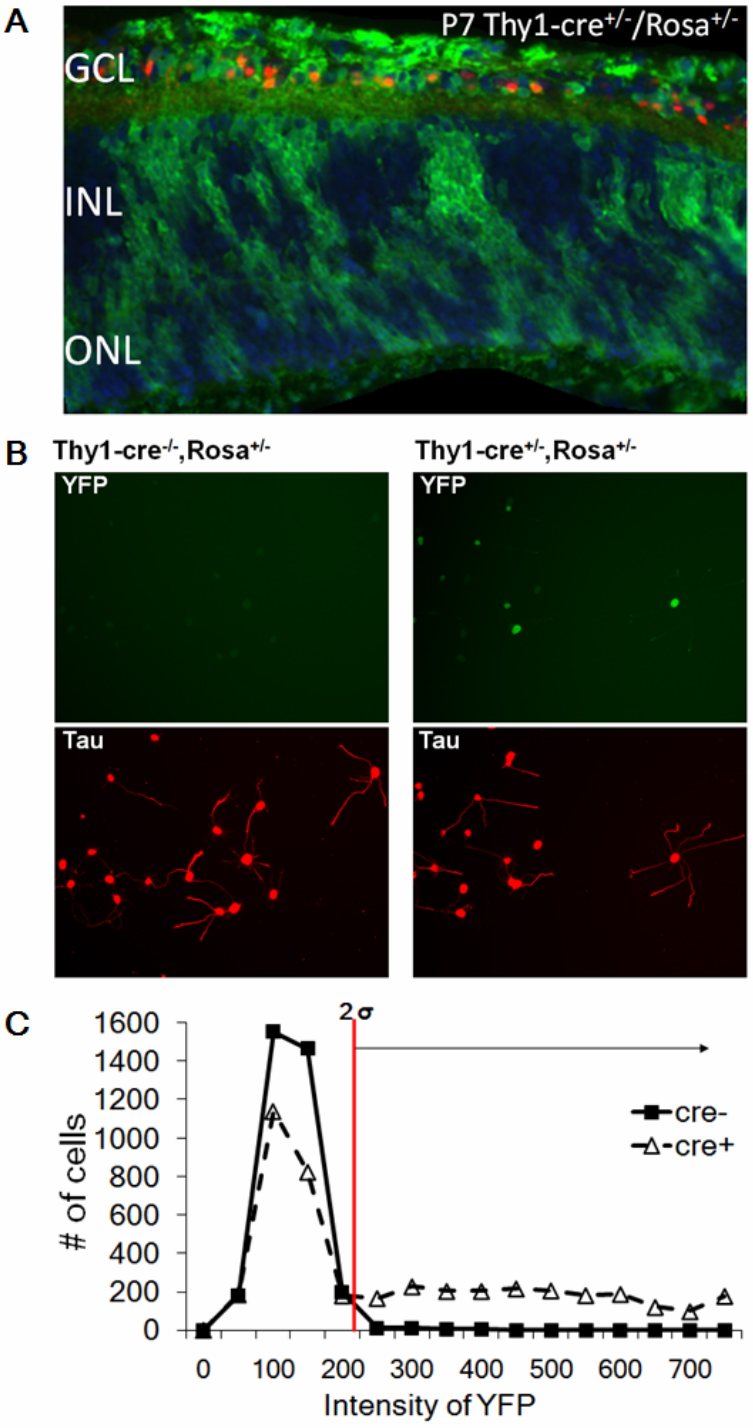

<u>Figure S6.</u> Half of RGCs activate Cre in the Thy1-cre$^{+/-}$/Rosa$^{+/-}$ mice. Alexa Fluor 594-labeled cholera toxin B was injected into the superior colliculus of P7 Thy1-cre$^{+/-}$/Rosa$^{+/-}$ mice to retrogradely label RGCs (red). Eyes were fixed, sectioned and immunostained to amplify the EYFP signal (green). A) Retinal cross sections reveal that YFP was expressed in RGCs, as well as in other retinal cells. B) RGCs from P10 Thy1-cre$^{+/-}$/Rosa$^{+/-}$ and Thy1-cre$^{-/-}$/Rosa$^{+/-}$ mice were purified by immunopanning, cultured on PDL- and laminin for 3 days, and immunostained for Tau (neurites) and GFP (to amplify YFP). Images were taken both with a Zeiss microscope and by the Cellomics Kineticscan software to determine intensity of YFP fluorescence. C) Two times the standard deviation of background intensity in Thy1-cre$^{-/-}$/Rosa$^{+/-}$ RGCs yielded a baseline threshold for "YFP +". 46% of RGCs were YFP +, suggesting that this Thy1-cre line is targeting approximately half of immunopanned RGCs.

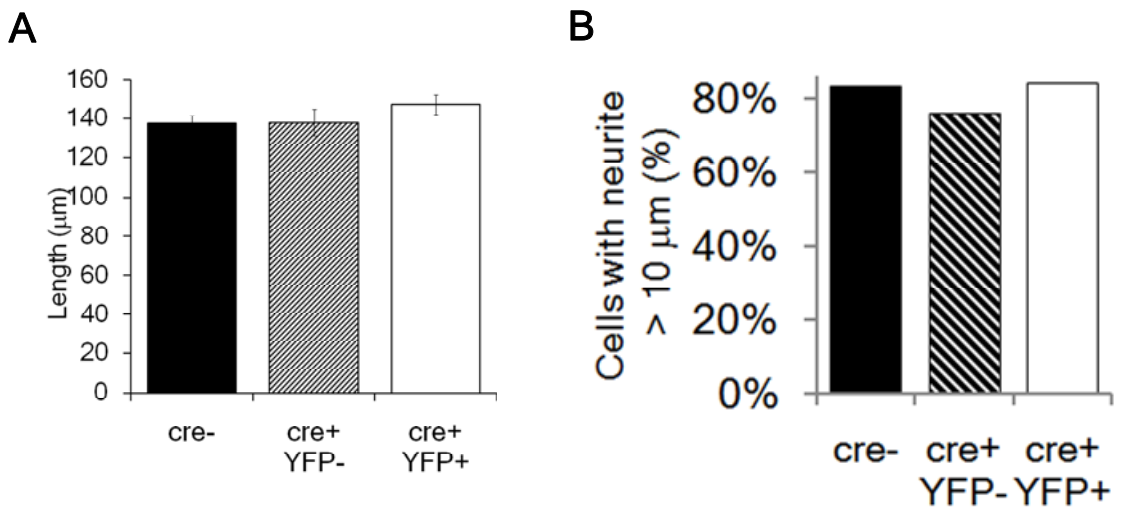

<u>Figure S7.</u> Transgenic Cre expression does not affect RGC neurite growth. RGCs from P10 Thy1-cre$^{+/-}$/Rosa$^{+/-}$ and Thy1-cre$^{-/-}$/Rosa$^{+/-}$ mice were purified by immunopanning, cultured on PDL and laminin for 3 days, and immunostained for Tau (neurites) and GFP (to amplify YFP). Cellomics Kineticscan software imaged and traced neurites, and measured YFP intensity. The baseline threshold of YFP intensity indicating cre targeting was determined as in Supplemental Figure 6, above. RGCs were grouped either as all RGCs from Thy1-cre- animals (no Cre expression, black bars), YFP- cells from Thy1-cre+ animals (also no Cre, hatched bars), or YFP+ cells from Thy1-cre+ animals (Cre-expressing RGCs, white bars). Neurons with growth <10 µm were not included in the length analysis. Quantification of total neurite length (A) or of percent of RGCs with at least one neurite >10 µm (B) revealed no differences between genotype (A: ANOVA revealed no significant differences between genotype; 1 representative experiment shown, n>2000 for each condition; mean ± SEM).

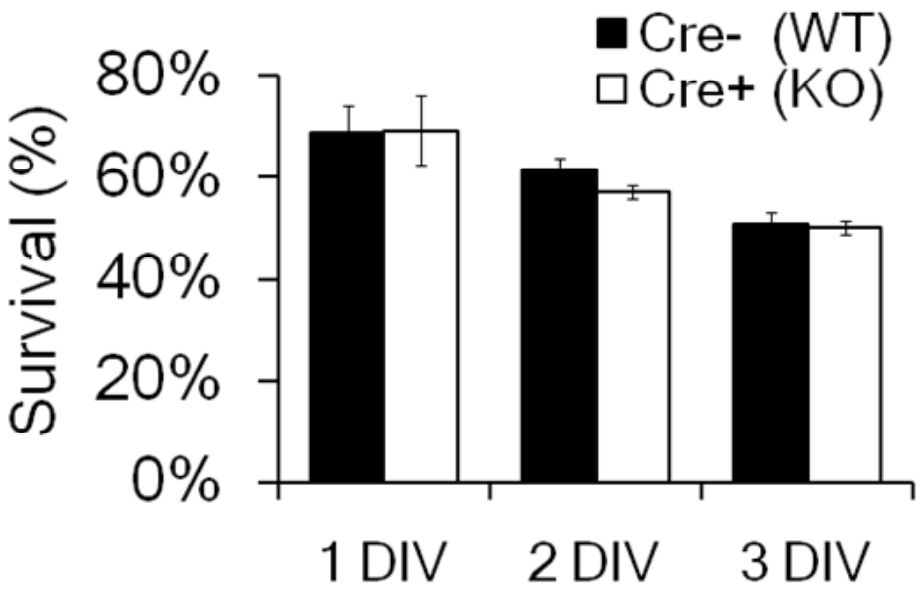

Figure S8. KLF4 knockout does not affect survival of RGCs in vitro. Purified P12 RGCs were cultured from Thy1-cre$^{-/-}$/KLF4$^{fl/fl}$/Rosa^{+} (Cre- WT) and Thy1-cre$^{+/-}$/KLF4$^{fl/fl}$/Rosa^{+} (Cre+ KO) mice. MTT survival assays at 1-3 DIV showed no significant differences in survival between KLF4 KO and WT RGCs (N=3; mean ± SEM).

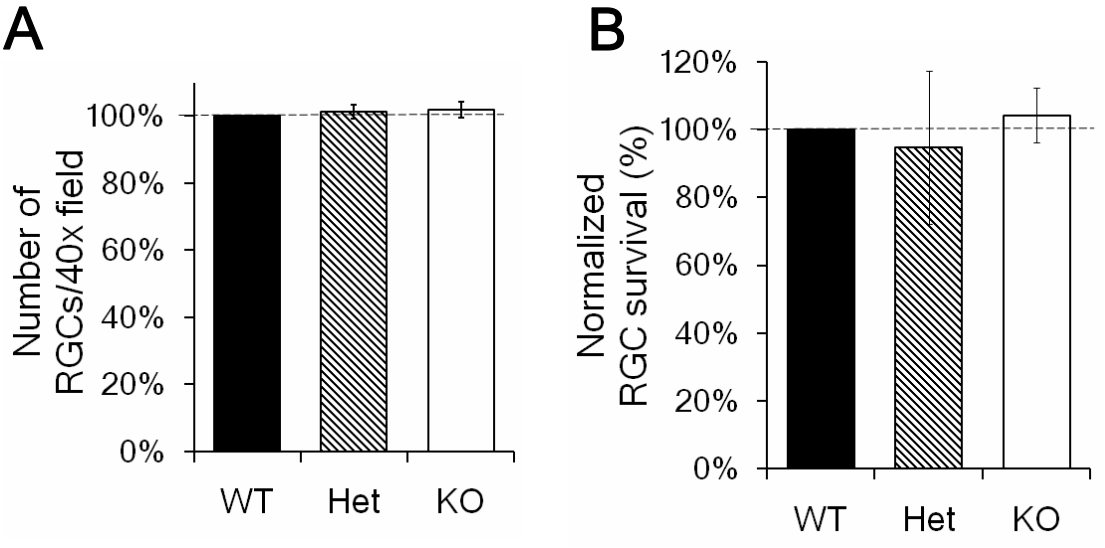

Figure S9. KLF4 knockout during development does not affect adult RGC number or survival after injury. Two weeks after optic nerve crush of Thy1-cre^{+}/KLF4$^{+/+}$ (WT), Thy1-cre^{+}/KLF4$^{fl/+}$ (Het), and Thy1-cre^{+}/KLF4$^{fl/fl}$ (KO) mice, retinas from both the control eye (uninjured nerve) and injured eye (crushed nerve) were flatmounted and immunostained for βIII tubulin (Tuj1) to label RGCs. Confocal imaging of retinas from knockout animals, normalized to WT, showed no differences in basal RGC number in the contralateral uninjured retinas (A; mean ± SEM; n=8 WT, 4 Het, 9 KO) or in RGC survival two weeks after optic nerve crush (B; mean ± SEM; n= 6 WT, 4 Het, 9 KO).

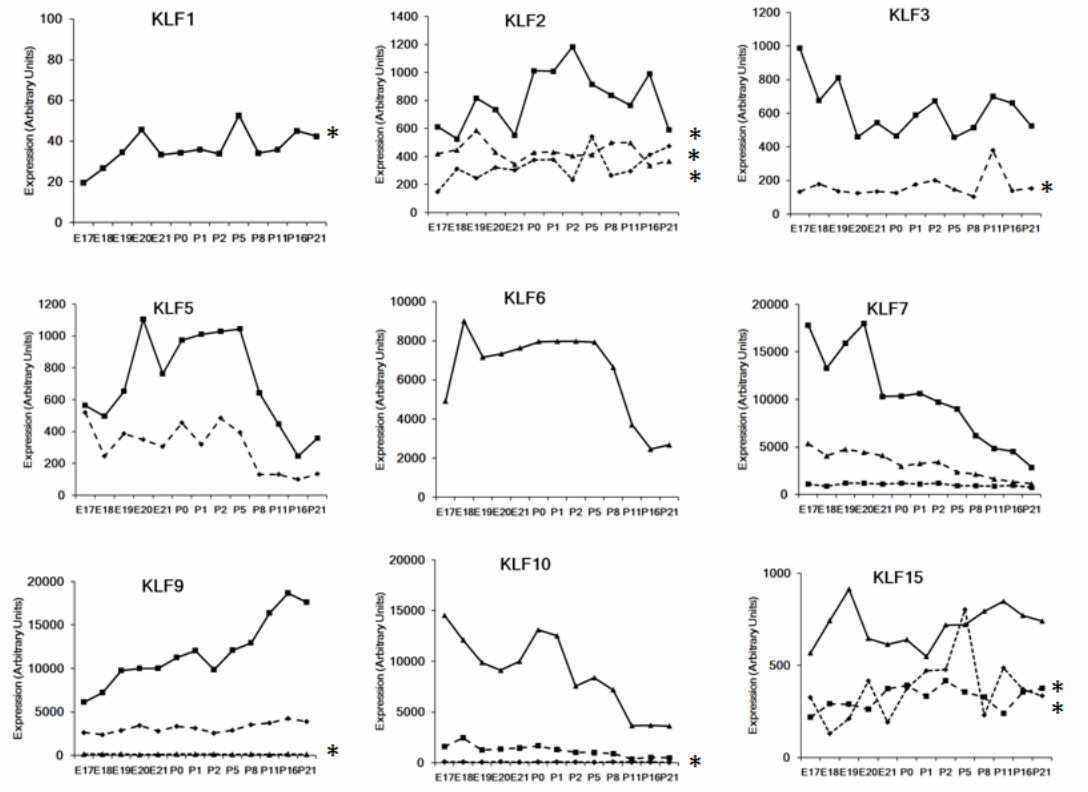

<u>Figure S10.</u> Multiple KLFs are expressed in RGCs and are developmentally regulated. RNA was isolated from acutely purified RGCs from multiple ages and analyzed by microarray analysis on Affymetrix chips (*1*). 9 of 17 KLFs were probed on these arrays using between 1-3 probes; probes not present in at least 2 samples within one age by the Affymetrix algorithm are marked as "absent" with an asterisk at the end of the line. Occasionally one probe would not detect message while the other probe would, as often happens in microarray datasets. All of these KLFs except for KLF1 were detected in RGCs by RT-PCR (Fig. 4).

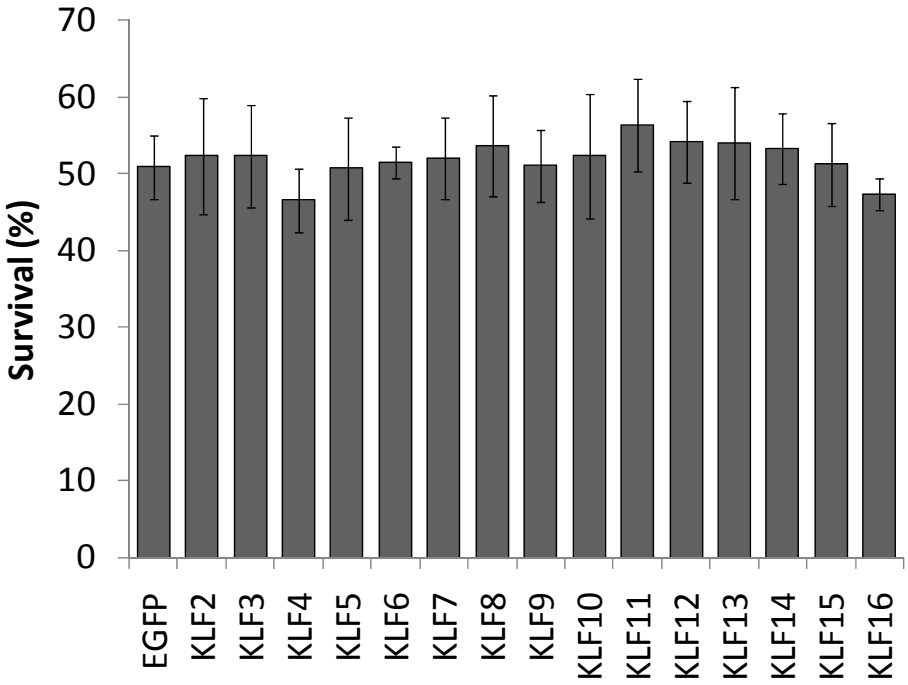

Figure S11. Overexpression of KLF transcription factors does not affect cell survival. P5 cortical neurons were dissociated, transfected with EGFP or KLFs, and cultured on PDL- and laminin- coated plates in growth media. After 72 hours, the percent of cells that excluded SYTOX orange dye was quantified (Cellomics Kineticscan). Transfection with KLFs did not significantly change neuronal survival ($p>0.50$, ANOVA with Dunnett's post-test; N=3, n>500; mean ± SEM).

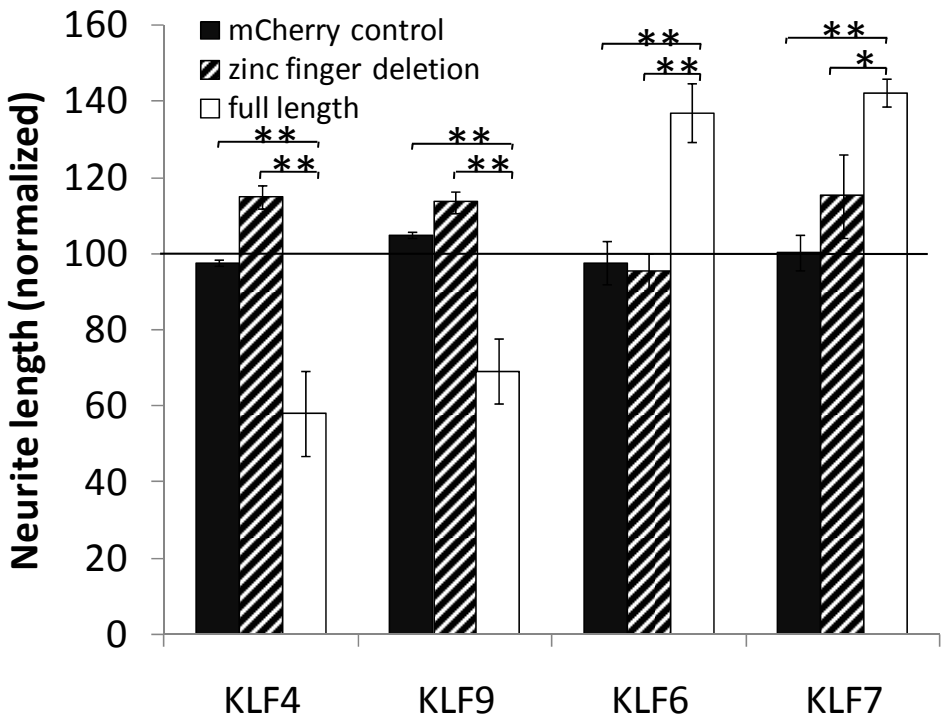

Figure S12. KLF-mediated regulation of neurite length in cortical neurons requires the C-terminal zinc finger DNA-binding domain. mCherry control, full length KLF-IRES-mCherry, or zinc finger deletion KLF-^C –IRES-mCherry constructs encoding KLF4, -9, -6, or -7 were transfected into P5 cortical neurons. Neurons were plated for 3 days on laminin and immunostained for beta-III tubulin. Bars represent average total neurite length (Cellomics KSR) of transfected (mCherry+) neurons. Compared to mCherry control-transfected neurons, full length but not truncated KLFs significantly affected neurite lengths. (N=3, n>100; * $p<0.05$, ** $p<0.01$, ANOVA with post hoc Dunnett's test; mean ± SEM).

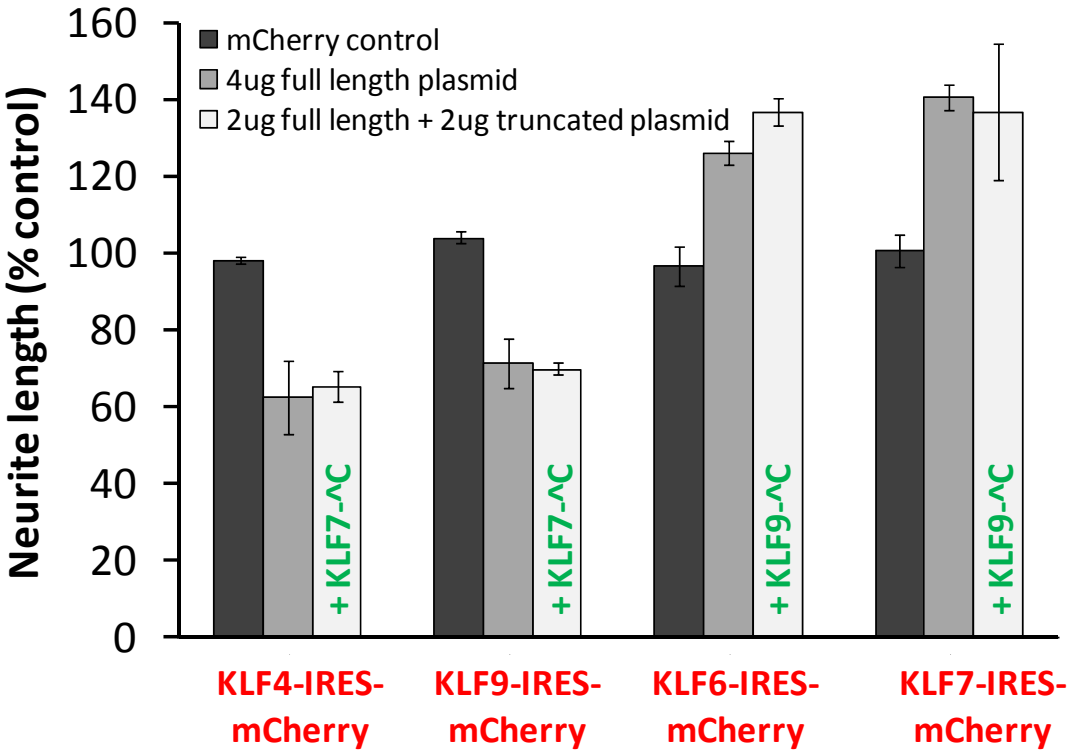

Figure S13. Effect of KLFs in combinatorial experiments is independent of µg of plasmid transfected. 4µg of control mCherry, 4µg of full length KLF–IRES-mCherry, or 2µg of full length KLF–IRES-mCherry plus 2µg of truncated (non-functional, see Fig. S12) KLF-^C –IRES-mCherry were transfected into P5 cortical neurons. Neurons were plated for 3 days on laminin and immunostained for beta-III tubulin. Bars represent average total neurite length (Cellomics KSR) of transfected (mCherry+) neurons. Neurons transfected with 4µg and 2µg of functional KLFs had similar neurite lengths (N=3, n>100; $p>0.05$, ANOVA with post hoc Dunnett's test; mean ± SEM).

Materials and Methods

Detailed protocols are available upon request.

Constructs for transfection

For the screen in hippocampal neurons, constructs in pEXPRESS-1, pSPORT or pCMV-SPORT6 (Open Biosystems) were co-transfected with pMAX (EGFP, Amaxa), and compared to an empty vector/pMAX co-transfection. The purchased constructs for the screen were full-length rat cDNAs (19/111, 17%), or else mouse (73%) or human (10%) when the full-length rat cDNA was unavailable.

Flag-tagged KLF4 constructs in a CS2+ vector were a generous gift of Chunming Liu (Univ of Texas). The flag control vector was purchased from Genecopoeia. Mouse KLF4 (Open Biosystems) and mCherry (gift of Roger Tsien, UCSD) were cloned into the pIRES2-eGFP vector (Clontech).

KLFs -1, -4, -5, -6, -7, -10, -12, -15, and -17 were obtained from Open Biosystems. KLF2 was a kind gift from Jerry Lingrel, Univ. of Cincinnati. The open reading frame of KLF9 was cloned from postnatal rat cortex, and KLFs -3, -8, -11, -13, -14, and -16 were cloned from mouse spleen or testis. All 17 KLFs were cloned into the CMV-pSPORT6 expression vector. pMAX (eGFP, Amaxa), or mCherry-pCMV-Sport6 were used as reporters in co-transfection experiments in cortical neurons.

For combinatorial experiments, the EGFP coding region of pIRES2-EGFP was replaced with mCherry. KLFs 4, -6, -7, and -9, and truncated versions that lacked the C-terminus zinc finger domain but maintained the adjacent NLS were cloned into both the IRES-EGFP and IRES-mCherry plasmids.

Culture and transfection of primary neurons

Hippocampal neurons - Embryonic day 18 (E18) rat hippocampi (Brainbits, LLC) were placed into Hibernate E media (Brainbits, LLC) containing 0.25% trypsin and 0.008% DNAse for 15 min at 37 deg C, washed 5 times with Hibernate E containing B27 (1:50), and triturated with variable sized fire-polished pipettes. Cells (500,000/tube) were pelleted (5 min, 80*g*), resuspended in Rat Neuron Nucleofector solution (Amaxa) containing 3.5 µg DNA, and electroporated (Amaxa, program G-13). Immediately following transfection, 500µl of growth media (see below) were added to transfected cells. Cells were plated onto PDL- and laminin-coated plates. A full media change was performed 4 hours following transfection. Transfection efficiencies were typically ~60%, and co-transfection efficiencies using 3 µg "gene-of-interest" DNA/0.5 µg reporter DNA were typically ~99%.

RGCs – Lipofectamine transfection - 400,000 embryonic RGCs purified by immunopanning (*2, 3*), were incubated with 2 µl Lipofectamine 2000 (Invitrogen) and 0.8 µg DNA for 15 min at 37 deg C, and then plated on PDL- and laminin-coated plates in RGC media (see below (*2*). A full media change was performed 4 hours following transfection. Transfection efficiencies were typically ~2%.
Electroporation – 100,000 postnatal RGCs were purified by immunopanning. Final cell pellets were resuspended in an electroporation solution containing 2µg of total DNA (GFP reporter and gene of interest), placed in a small cell number cuvette (Amaxa) and

electroporated using Amaxa program SCN#1. Immediately following electroporation, growth media was added to the mixture and the whole solution placed into a small Eppendorf tube. RGCs were centrifuged for 16 minutes at 1800 rpm prior to resuspension and plating.

Cortical neurons - Frontal cortex from P5 rats was dissociated sequentially in papain and trypsin. Dissociated cells were co-transfected with plasmid DNA-encoding KLFs and mCherry reporter at a 1:6 ratio, using electroporation in a 96-well format (*4*). Cells were plated in PDL- and laminin-coated 96-well plates in growth media conditioned overnight by astroglial cultures (*5*). Transfection efficiencies were typically ~20%, and co-transfection efficiencies were typically >90%. For experiments combining KLFs, 2µg of KLF-IRES-mCherry and 2µg of KLF-IRES-EGFP plasmid were co-transfected. Only neurons that expressed both mCherry and EGFP were included in the analysis of neurite lengths.

Growth media - The culture media for RGCs, hippocampal and cortical neurons was modified from (*2*), and included Neurobasal, penicillin/streptomycin, insulin (5µg/ml), sodium pyruvate (1mM), transferrin (100µg/ml), BSA (100µg/ml), progesterone (60ng/ml), putrescine (16µg/ml), sodium selenite (40ng/ml), triiodo-thyronine (T3, 1ng/ml), L-glutamine (1mM), N-acetyl cysteine (NAC, 5µg/ml), forskolin (5mM) and B27 (*6*). Media for RGCs and hippocampal neurons also contained BDNF (50ng/ml) and CNTF (10ng/ml); media for embryonic RGCs also contained GDNF (40ng/ml); media for electroporated RGCs also contained both GDNF and bFGF (10ng/ml).

Immunostaining

For cultured neurons, cultures were fixed using pre-warmed (37 deg C) 4% paraformaldehyde (PFA). Following rinses in PBS, cultures were blocked and permeabilized in 20% normal goat serum (NGS)/0.02% triton X-100 in antibody buffer (150mM NaCl, 50mM Tris base, 1% BSA, 100mM L-Lysine, 0.04% Na azide, pH 7.4) for 30 min to reduce non-specific binding. Cultures were incubated overnight at 4 deg C in antibody buffer containing primary antibodies, washed with PBS, incubated in antibody buffer containing secondary antibodies and DAPI for 4 hours at room temperature, washed with PBS, and left in PBS for imaging.

For whole-mount staining, retinas from PFA-perfused animals were immunostained as above with the following modifications: all incubations were performed on a rocker, and the secondary antibody incubation was performed overnight at 4 deg C. Retinas were mounted in mounting medium with DAPI (Vectashield) on coverslips for confocal imaging.

Primary antibodies used for these experiments included anti-Tau (1:200, Sigma, T6402) anti-FLAG (1:750, F1804, Sigma), anti-GFP (1:600, Aves Labs, GFP-1020), anti-MAP2 (1:10,000, Abcam, ab5392; 1:150, Sigma, M1406), anti-Turbo GFP (1:10,000, Evrogen, AB513), and anti-beta-III-tubulin (Tuj1, 1:400, Covance, MMS-435P; 1:500, Sigma, T3952). Secondary antibodies were Alexa Fluor-488, -594, or -647-conjugated, highly cross-adsorbed antibodies (Invitrogen).

Quantification of neurite length

For "High Content Analysis" (also called High Content Screening, or HCS) of neuronal morphology, including neurite length, dendrite length, neurite number and neurite branching, automated microscopes (Cellomics KSR or VTI) and image analysis software (Cellomics BioApplications) were used to image and trace neurons using a 5x or 10x objective following immunostaining. Cortical neurons were traced using βIII tubulin immunoreactivity to visualize neurites. RGCs were traced using antibody-amplified EGFP signal, which filled transfected neurites. In the case of RGCs, neurons with dim EGFP label in neurites were excluded from analysis, due to frequent tracing errors of faint processes; the threshold for exclusion was established using a population of control neurons. Images and tracing were spot-checked to verify that the algorithms were correctly identifying neurites and quantifying growth.

For those experiments requiring hand tracing, including confirmations of automated quantification, surviving neurons were identified by nuclear morphology and DAPI intensity and imaged in multiple fluorescent channels using a Zeiss Axiovert 200M microscope. Hand tracing was performed using Axiovision software. MAP2+ neurites, which typically demonstrated thicker origins and tapering widths, were measured as dendrites; Tau+/MAP2- neurites, which typically demonstrated thinner, non-tapering profiles, were measured as axons.

Quantification of neuronal survival

Survival of neurons was determined using either an MTT (3-(4,5-dimethylthiazol-2-yl)-2,5-diphenyl tetrazolium bromide) assay (*7*), identification of dead nuclei by the Cellomics software (see below), or Sytox staining. MTT (.5 mg/ml) was applied to at least 3 wells per condition and incubated at 37 deg C for 30 min. Surviving neurons produced a blue precipitate; dead neurons remained colorless. At least 3 wells per condition and multiple fields of view in identical well locations were counted for each sample using a grid overlay.

To determine survival using Cellomics HCS assays, DAPI nuclear staining morphology was used. Dead cells had a higher DAPI intensity per pixel and smaller nuclei; surviving cells had low DAPI fluorescence intensity per pixel and a larger nucleus. Multiple fields of view per well were counted for each sample, with a typical replicate being 6 wells within an experiment.

Cortical neuron survival after transfection was measured by simultaneous Hoechst and Sytox orange dye staining at 1 or 3 days after plating. Hoechst+/Sytox– (surviving) cells were quantified with the Cellomics KSR, with a minimum of 500 cells counted per treatment.

Quantitative reverse transcription polymerase chain reaction (qRT-PCR)

RGCs were purified by immunopanning as above and the pellet from the final centrifugation (before any cell culture) was snap frozen in liquid nitrogen. In most cases, multiple pellets (preps) were combined for each sample. RNA was purified (RNeasy, Invitrogen), subjected to reverse transcription (RT, iScript, Bio-Rad), and the resulting cDNA was used as the template for a quantitative-PCR reaction (Sybr green, Bio-Rad) performed on an iCycler (Bio-Rad) with KLF-X and 18S primers. In most tests, 6 repeat

wells (technical replicates) were used for each condition. "No RT" control samples were also tested. To determine fold change, an efficiency analysis was performed for each tissue type in combination with the specific primers being tested. Dilutions of a sample were made for 1:10, 1:100, and 1:1000, and the threshold counts graphed as a line, with the slope being used for the efficiency formula (*8*). Each experiment was performed 2-3 times with different pools of RNA (biological replicates).

For non-quantitative RT-PCR, RGC RNA was purified and reverse-transcribed as described above. 1 µl of cDNA was used as a template for each PCR reaction (Phusion, NEB). 5 µl of this product was run on a 2% agarose gel containing Gel Red (Biotium, Hayward CA), and visualized using Gene Genius gel documentation system (Syngene, Frederick, MD). The experiment was repeated to confirm initial band expression using RNA from a separate set of animals (biological replicates).

Primers used for genotyping N-Tg(Thy1-cre)1Vln/J mice (Jackson Laboratories) and Gt(ROSA)26Sor$^{tm1(eYFP-Cos)}$ mice (Jackson Laboratories), were according to the Jackson Laboratories recommendations (available on their website), as follows:
Cre – oIMR0042 ctaggccacagaattgaaagatct,
oIMR0043 gtaggtggaaattctagcatcatcc,
oIMR1084 gcggtctggcagtaaaaactatc,
oIMR1085 gtgaaacagcattgctgtcactt;
Rosa – oIMR0316 ggagcgggagaaatggatatg,
oIMR0883 aaagtcgctctgagttgttat,
oIMR4982 aagaccgcgaagagtttgtc.
fKLF4 mice were genotyped as described (*9*). The rd mutation was assayed through genotyping as described (*10*). For qRT-PCR, primers for KLF4 were as described (*11*); for rat KLF6 were forward: gagttcctcggtcatttcca, reverse: tgctttcaagtgggagcttt; for rat KLF7 were forward: ttgctctctcgggacaagtt, reverse: gagctgagggaagccttctt; for rat KLF9 were forward aacaaataccgacccatcca, reverse: agactttcccacagccactg. For RT-PCR, primers for KLF1-KLF13 and KLF15-17 were as described (*12*) and for KLF14 were as described (*13*).

Animals

All use of animals conformed to the ARVO Statement for the Use of Animals in Research, and was approved by the Institutional Animal Care and Use Committee and the Institutional Biosafety Committee of the University of Miami.

Sprague-Dawley rats of varying ages were obtained from Harlan Laboratories.

Mice were bred from the following strains: floxed KLF4 (fKLF4) mice (*9*), B6.129X1-*Gt(ROSA)26Sort*$^{tm1(EYFP)Cos}$/J (Stock #006148, Jackson Laboratory), and FVB/N-Tg(Thy1-cre)1Vln/J (Stock#006143, Jackson Laboratory). The Thy1-cre background strain, FVB, was homozygous for retinal degeneration (rd) mutations, and this mutation was bred out using C57BL/6J as detected through genotyping (*10*). Once the rd mutation was bred out, we spot checked the rd genotype to confirm periodically that the mutation was absent.

Intraorbital Optic Nerve Crush and Intravitreal Injection

For all in vivo experiments, optic nerve crush, tissue processing, imaging and analysis were performed masked, such that the experimenters did not know the genotype of the animal at any stage until the analysis was complete. In separate experiments looking at shorter term post-crush survivals, we saw no spared axons greater than 0.2 mm beyond the crush site (Y. Hu, A. Peterson, J. Bixby and J. Goldberg, data not shown). In this manuscript, any axon sparing would be expected to be distributed randomly between groups, due to the masked design.

8-12 week old Thy1-cre^{+}/KLF4$^{+/+}$, Thy1-cre^{+}/KLF4$^{fl/+}$, Thy1-cre^{+}/KLF4$^{fl/fl}$ littermate mice were used for optic nerve crush experiments. Following induction of anesthesia, the left intraorbital optic nerve was surgically exposed, the dural sheath was opened longitudinally, and the nerve was crushed 1 mm behind the eye with angled jeweler's forceps (Dumont # 5) for 10 sec, avoiding injury to the ophthalmic artery. Nerve injury was verified visually at the crush site, while the vascular integrity of the retina was evaluated by fundoscopic examination. Mice with any significant postoperative complications (e.g., retinal ischemia, cataract) were excluded from further analysis. For anterograde axon labeling, intravitreal injections of 1 µl cholera toxin subunit B (CtB594, 10µg/µl; Molecular Probes) were performed just posterior to the pars plana with pulled glass pipette connected to a 50 µl Hamilton syringe. Care was taken not to damage the lens. One day later, at 2 weeks after the crush injury, mice were deeply anaesthetized and perfused with 4% PFA in 0.1 M phosphate buffer. Optic nerves and retinas were dissected and post-fixed in 4% PFA for one hour and subsequently washed in PBS. Optic nerves were incubated in 30% sucrose at 4 degrees overnight prior to mounting in OCT. Longitudinal sections (16 µm) were made of the entire optic nerve. All sections with an apparent crush site and CtB labelling were imaged with a 20x objective. Pictures were taken, starting with the furthest regenerating axons and working backwards toward the crush site. Lines were drawn perpendicular to the long axis of the optic nerve 0.2, 0.3, 0.5, 0.75, 1, and 1.5 past the crush site (as applicable), and CtB+ axons between these lines were counted. Analysis of the total sum of regenerating fibers from all sections for each animal were performed as well as the average number of axons at each measurement location/distance per number of sections. Using either analysis, the data yielded the same results.

Statistical analysis. Distance and fiber-sum data were log transformed to effect linearity (a basic assumption of the statistical tests used) and approximate normality of residuals. As some fiber-sum measurements were zero, a small positive constant, 0.2, was added to all fiber-sum measurements prior to taking the logarithm. An analysis of covariance, with a mixed model component to account for multiple measurements in the same animals, was used to compare the distance relationship of fiber-sums by genotype between the groups. A second analysis in which zero values were excluded reached similar conclusions.

Retinal Survival Quantification

Eyes were dissected from PFA-perfused animals and left in 4% PFA for an additional hour. Retinas were then dissected into PBS to await immunostaining. Whole-mount immunostaining was performed (see above) using anti-beta-III tubulin (Tuj1) to visualize

RGCs, and DAPI to detect nuclei. Retinas were mounted onto coverslips in mounting medium (Vectashield) and imaged on a Leica confocal microscope. Using a 40x oil objective, 4 stacked images were taken 2 fields of view from the optic disc in each perpendicular direction. RGCs were quantified by an observer masked to genotype using Metamorph software.

References for Supplementary Data

1. J. T. Wang *et al.*, *J Neurosci* **27**, 8593 (2007).
2. A. Meyer-Franke, M. R. Kaplan, F. W. Pfrieger, B. A. Barres, *Neuron* **15**, 805 (1995).
3. B. A. Barres, B. E. Silverstein, D. P. Corey, L. L. Chun, *Neuron* **1**, 791 (1988).
4. W. J. Buchser, J. R. Pardinas, Y. Shi, J. L. Bixby, V. P. Lemmon, *Biotechniques* **41**, 619 (2006).
5. M. J. De Hoop, L. Meyn, C. G. Dotti, *Culturing hippocampal neurons and astrocytes from fetal rodent brain.* . J. E. Celis, Ed., Cell biology: a laboratory handbook (Academic, San Diego, ed. 2, 1998).
6. Y. Chen *et al.*, *J Neurosci Methods* **171**, 239 (2008).
7. T. Mosmann, *J Immunol Methods* **65**, 55 (1983).
8. M. W. Pfaffl, *Nucleic Acids Res* **29**, e45 (2001).
9. J. P. Katz *et al.*, *Development* **129**, 2619 (2002).
10. E. Gimenez, L. Montoliu, *Lab Anim* **35**, 153 (2001).
11. A. Suzuki *et al.*, *Exp Biol Med (Maywood)* **231**, 632 (2006).
12. S. A. Eaton *et al.*, *J Biol Chem* **283**, 26937 (2008).
13. S. Scohy *et al.*, *Genomics* **70**, 93 (2000).